HEALTH AND MEDICINE

Deconstruction of an African folk medicine uncovers a novel molecular strategy for therapeutic potassium channel activation

Angele M. De Silva*, Rían W. Manville*†, Geoffrey W. Abbott†

A third of the global population relies heavily upon traditional or folk medicines, such as the African shrub *Mallotus oppositifolius*. Here, we used pharmacological screening and electrophysiological analysis in combination with in silico docking and site-directed mutagenesis to elucidate the effects of *M. oppositifolius* constituents on KCNQ1, a ubiquitous and influential cardiac and epithelial voltage-gated potassium (Kv) channel. Two components of the *M. oppositifolius* leaf extract, mallotoxin (MTX) and 3-ethyl-2-hydroxy-2-cyclopenten-1-one (CPT1), augmented KCNQ1 current by negative shifting its voltage dependence of activation. MTX was also highly effective at augmenting currents generated by KCNQ1 in complexes with native partners KCNE1 or SMIT1; conversely, MTX inhibited KCNQ1-KCNE3 channels. MTX and CPT1 activated KCNQ1 by hydrogen bonding to the foot of the voltage sensor, a previously unidentified drug site which we also find to be essential for MTX activation of the related KCNQ2/3 channel. The findings elucidate the molecular mechanistic basis for modulation by a widely used folk medicine of an important human Kv channel and uncover novel molecular approaches for therapeutic modulation of potassium channel activity.

INTRODUCTION

Essential modern medicines are estimated by the World Health Organization to be readily available to two-thirds of the global population, with the remainder relying on traditional or folk remedies to treat many serious illnesses and ailments (*1*). Extracts from the leaf of *Mallotus oppositifolius* (Fig. 1A), a shrub commonly found in Ghana and Nigeria (*2*, *3*), reportedly have anti-inflammatory and antimicrobial properties, and are used to treat epilepsy, diabetes, headaches, pain, parasitic eye infections, kidney infections, and paralysis (*3*, *4*).

One of the primary components of *M. oppositifolius* leaf extract, mallotoxin (MTX; also known as rottlerin), was previously reported to activate BK, hERG, and KCNQ1 potassium channels (*5*–*7*). However, the binding sites, and therefore direct versus indirect mechanism for this activation, have not previously been elucidated. Furthermore, the potential effects of other *Mallotus* components on BK, hERG, and KCNQ1 have not been elucidated. Human KCNQ1 is ubiquitously expressed in tissues including the heart, gastrointestinal tract, thyroid, pancreas, pituitary gland, choroid plexus, kidney, and inner ear (*8*) and is highly influential in human health. *KCNQ1* gene variants have been linked to cardiac arrhythmias (*8*, *9*), deafness (*10*), diabetes (*11*–*13*), anemia, gastric hyperplasia, and gastric tumors (*14*, *15*). *Kcnq1* germ line deletion in mice also causes thyroid dysfunction (*16*) and its pharmacological disruption results in renal abnormalities (*17*). Kv channels such as KCNQ1 are composed of tetramers of α subunits each containing six transmembrane segments (S1 to S6), split into a voltage-sensing domain (VSD) (S1 to S4) and a pore module (S5 and S6) (Fig. 1B). KCNQ1 is versatile, not only serving physiological roles such as repolarizing excitable cells including cardiac myocytes but also providing a K^+ recycling pathway in nonexcitable, polarized epithelial cells such as parietal cells, facilitating gastric acid secretion. This versatility is possible because KCNQ1 forms complexes with single transmembrane domain KCNE ancillary (β) subunits, resulting in channels with diverse functional and pharmacological characteristics (*8*).

Because the ubiquity and importance of KCNQ1 make it a strong candidate for explaining the underlying mechanistic basis of the therapeutic effects of *Mallotus*, we screened leaf extract components for KCNQ1 activity. We found that two components, MTX and 3-ethyl-2-hydroxy-2-cyclopenten-1-one (CPT1), activate KCNQ1 channels by an unexpected, novel mechanism—binding to a novel drug site at the foot of the voltage sensor.

RESULTS

M. oppositifolius leaf extract components activate KCNQ1

We screened 10 previously identified *M. oppositifolius* leaf extract components (Fig. 1C) (*18*) by quantifying their effects on KCNQ1 tail currents at −30 mV immediately following channel activation at voltages between −80 and +40 mV using two electrode voltage clamp of KCNQ1 heterologously expressed in *Xenopus laevis* oocytes. We found that 2 of the 10 compounds studied, CPT1 and MTX, negatively shifted the voltage dependence of KCNQ1 activation, thus augmenting currents (Fig. 1C). MTX was the most potent and efficacious KCNQ1 activator. MTX activation of KCNQ1 was voltage dependent, with greater efficacy observed at hyperpolarized voltages (Fig. 1, D and E). CPT1 (100 μM) negatively shifted the voltage dependence of KCNQ1 activation by −5 mV. The other compounds had no effect at 30 or 100 μM on KCNQ1 current magnitude or other properties (Fig. 1, D and E, and figs. S1 and S2).

At −40 mV, 30 μM MTX increased KCNQ1 current 5.4-fold (Fig. 2, A and B); the activation EC_{50} (median effective concentration) was 9.9 ± 0.4 μM (Fig. 2B). At 100 μM, MTX caused a −27 mV negative shift in the voltage dependence of KCNQ1 activation, and the dose response for the $\Delta V_{0.5}$ activation was 9.4 ± 0.1 μM MTX (Fig. 2C). MTX speeded KCNQ1 activation and slowed its deactivation, suggesting stabilization of the KCNQ1 open state and destabilization of its closed state (fig. S2D). CPT1 was slightly less efficacious but 100-fold more potent, increasing KCNQ1 current 2.7-fold at −60 mV (100 μM) (Fig. 2, D

Bioelectricity Laboratory, Department of Physiology and Biophysics, School of Medicine, University of California, Irvine, Irvine, CA, USA.
*These authors contributed equally to this work.
†Corresponding author. Email: abbottg@uci.edu (G.W.A.); rmanvill@uci.edu (R.W.M.)

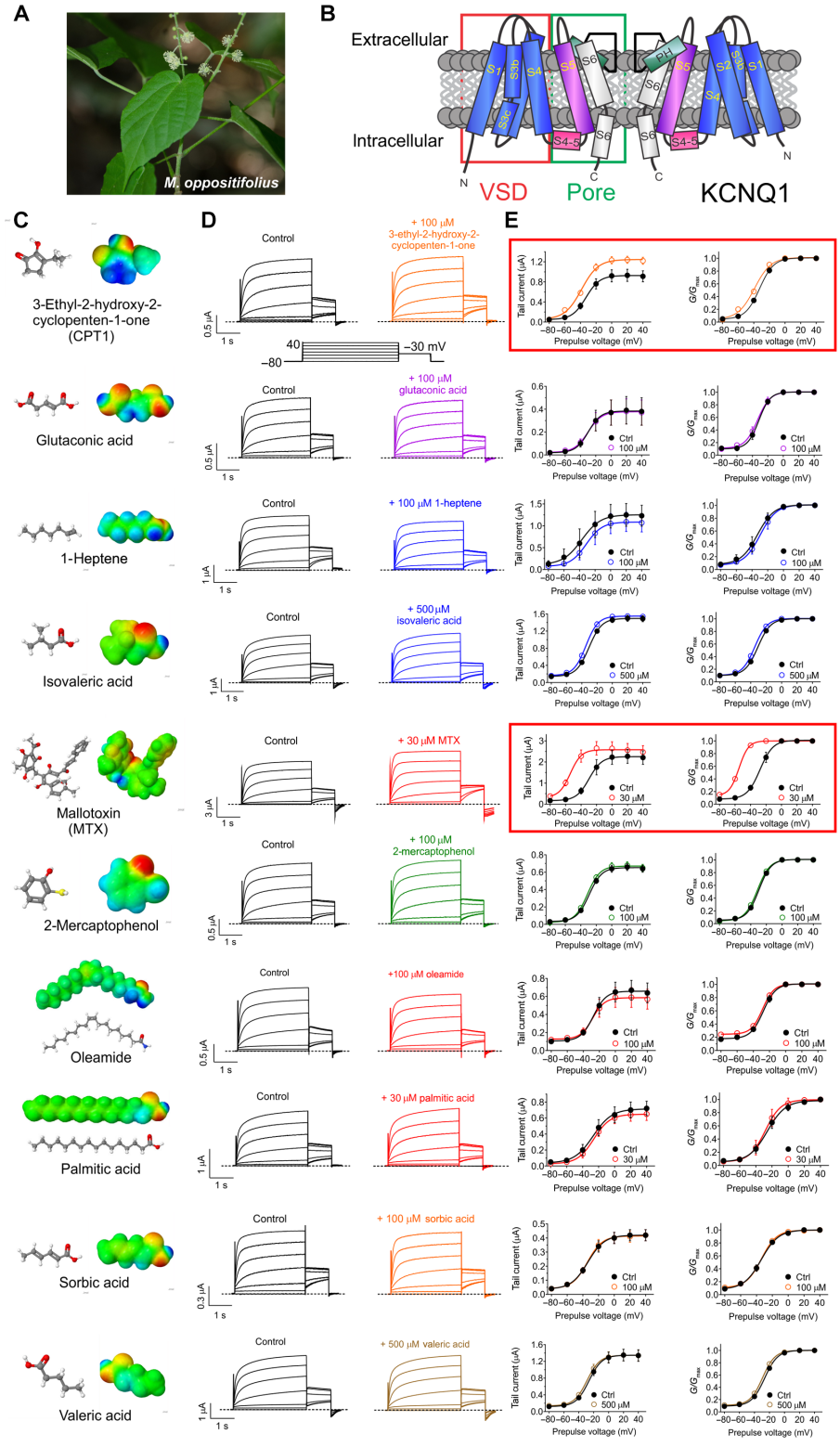

Fig. 1. Two components of *M. oppositifolius* leaf extract activate KCNQ1 channels. (**A**) *M. oppositifolius* (Geiseler) Mull. Arg. Photo by E. Bidault. Source: Tropicos.org. Missouri Botanical Garden (http://tropicos.org/Image/100521734). (**B**) KCNQ1 topology (two of four subunits shown). (**C**) Structure and electrostatic surface potential (blue, positive; green, neutral; red, negative) of *M. oppositifolius* leaf extract components. (**D**) Averaged KCNQ1 current traces in response to voltage protocol (upper inset) when bathed in the absence (control) or presence of *M. oppositifolius* leaf extract components (n = 5 to 8). Dashed line indicates zero current level in these and all following current traces. (**E**) Mean effects of leaf extract components [as in (D); n = 5 to 8] on KCNQ1 raw tail currents at –30 mV after prepulses as indicated (left); G/G_{max} calculated from tail currents (right). Error bars indicate SEM. Ctrl, control.

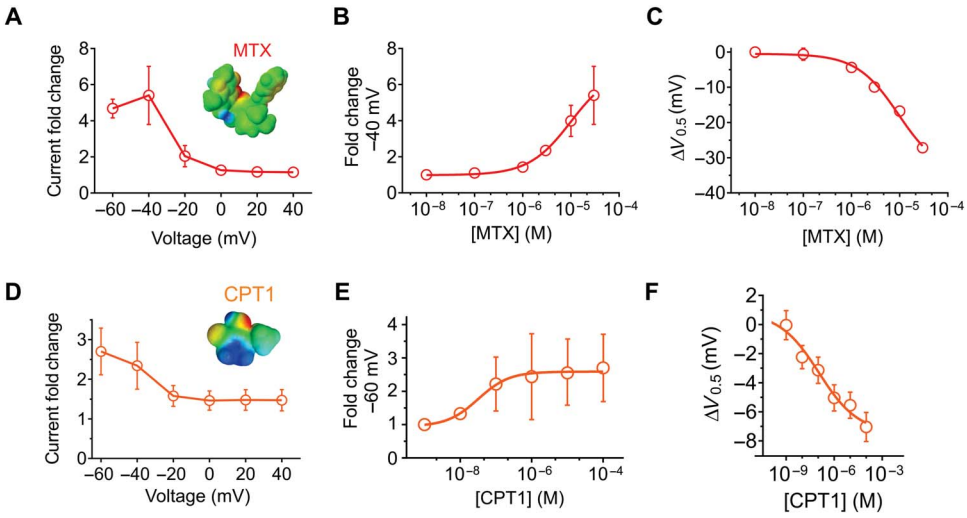

Fig. 2. MTX and CPT1 each activate KCNQ1 channels. All error bars indicate SEM. (**A**) Voltage dependence of KCNQ1 current fold increase by MTX (30 μM), plotted from traces as in Fig. 1 (n = 7). (**B**) Dose response of KCNQ1 channels at −40 mV for MTX (calculated EC_{50} = 10 μM; n = 7). (**C**) Dose response for mean $\Delta V_{0.5}$ of activation induced by MTX for KCNQ1 (n = 7). (**D**) Voltage dependence of KCNQ1 current fold increase by CPT1 (100 μM), plotted from traces as in Fig. 1 (n = 4 to 6). (**E**) Dose response of KCNQ1 channels at −60 mV for CPT1 (n = 4 to 6). (**F**) Dose response for mean $\Delta V_{0.5}$ of activation induced by CPT1 for KCNQ1 (n = 4 to 6).

and E); the activation EC_{50} was 0.09 ± 0.6 μM at −60 mV (Fig. 2E). CPT1 only shifted KCNQ1 activation $V_{0.5}$ by −6.4 mV, partly because its effects were less voltage dependent than those of MTX; the EC_{50} for the $\Delta V_{0.5}$ activation was 0.1 ± 0.8 μM CPT1 (Fig. 2F). CPT1 had less dramatic effects than MTX on KCNQ1 gating kinetics, yet still induced a statistically significant speeding of activation and slowing of deactivation (fig. S1D).

Interacting proteins alter KCNQ1 efficacy and sensitivity to MTX

KCNQ1 is regulated extensively by KCNE β subunits in vivo. In human ventricular myocardium, KCNQ1-KCNE1 channel complexes generate the slow-activating, noninactivating I_{Ks} current that is important for cardiac myocyte repolarization; the same channel complex is required for K^+ secretion into the endolymph of the inner ear (*19*). KCNE1 has been shown previously to both sensitize (*20*) and desensitize (*21*) KCNQ1 to various synthetic compounds. Here, MTX (30 μM) strongly augmented KCNQ1-KCNE1 currents across the voltage range tested and shifted the $V_{0.5}$ of activation by −45 mV, compared to the −27 mV shift in KCNQ1 activation voltage dependence induced by 30 μM MTX (Fig. 3, A and B, fig. S3). This, combined with the slowing of deactivation produced by MTX, induced a constitutively active component to the KCNQ1-KCNE1 current (because the channels did not close to any great extent between depolarizing pulses) (Fig. 3, A, C, and D), an effect we did not observe for MTX with homomeric KCNQ1 (Fig. 1D). However, the MTX EC_{50} for KCNQ1-KCNE1 (27.9 ± 0.3 μM; Fig. 3E) was threefold higher than that of KCNQ1 (9.9 ± 0.4 μM; Fig. 2B).

In contrast to KCNE1, KCNE3 converts KCNQ1 to a constitutively active channel by locking open the VSD, which in turn holds open the pore (*22*, *23*). KCNQ1-KCNE3 channels are thought to be important for regulating cAMP (adenosine 3′,5′-monophosphate)–stimulated chloride secretion in the intestinal epithelia (*24*). KCNQ1-KCNE3 channels were moderately inhibited, not activated, by 30 μM MTX across the voltage range studied (Fig. 3, F and G). KCNE4 is the most highly expressed KCNE subunit in human heart (*25*, *26*). In mouse heart, KCNE4 regulates Kv4 and Kv1.5 channels (*27*). KCNE4 strongly inhibits KCNQ1 activity in heterologous expression studies (*28*, *29*), although the role of this regulation in vivo is not known. MTX (30 μM) induced minor augmentation of KCNQ1-KCNE4 activity; therefore, it did not substantively interfere with KCNE4 inhibition of KCNQ1 (Fig. 3, H and I).

KCNQ1 can also form complexes with the Na^+-coupled myo-inositol transporter SMIT1 (encoded by *SLC5A3*). Complex formation results in reciprocal regulation of both KCNQ1 and SMIT1, and KCNQ1-SMIT1 complexes in the choroid plexus epithelium are important for regulating cerebrospinal fluid myo-inositol content (*8*). We previously showed that SMIT1 interacts with the KCNQ1 pore module, altering its conformation and, thus, relative ion permeability (Fig. 4, A and B) (*30*). Here, MTX (30 μM) negative shifted the voltage dependence of KCNQ1-SMIT1 activation by a similar extent to effects on KCNQ1 alone (Fig. 4, C to E, and fig. S4). The potency and efficacy of MTX on KCNQ1-SMIT1 were similar to those for KCNQ1 (Fig. 4F). However, MTX effects superimposed on those of SMIT1, which also negative shifts the voltage dependence of KCNQ1 activation; thus, KCNQ1-SMIT1 complexes with MTX were much more active at hyperpolarized membrane potentials than KCNQ1 channels with MTX (Fig. 4G). In summary, the data predict that MTX would be particularly effective at augmenting activity of KCNQ1 in vivo when in complexes with KCNE1 or SMIT1.

MTX influences pore conformation and is still active in high extracellular K^+

MTX effects on KCNQ1 were preserved in high (50 mM) extracellular K^+ (fig. S5, A and B), leading us to hypothesize that MTX might be positioned outside the pore, versus an internal pore location for MTX, a position in which high extracellular K^+ would be expected to knock it off. UCL2077 is a subtype-specific KCNQ open-channel blocker (*31*) thought to bind to and stabilize KCNQ1 S6 in the closed state without affecting S4 movement (*32*). UCL2077 also enhances KCNQ3 currents

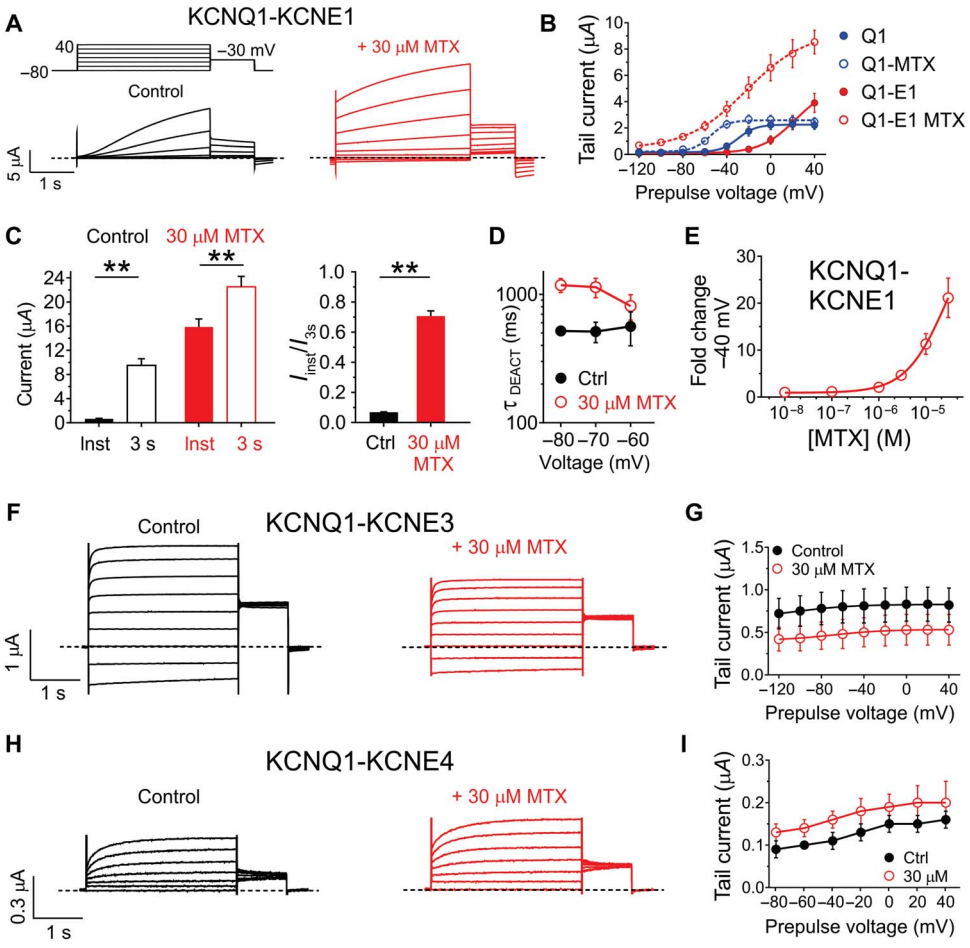

Fig. 3. KCNEs alter MTX effects on KCNQ1. All error bars indicate SEM. (**A**) Averaged KCNQ1-KCNE1 current traces in response to voltage protocol (upper left inset) in the absence (control) or presence of 30 μM MTX (n = 5). Dashed line indicates zero current level in this and all following current traces. (**B**) Mean effects of 30 μM MTX on KCNQ1 and KCNQ1-KCNE1 raw tail currents at −30 mV after prepulses as indicated [as in (A); n = 5]. (**C**) Mean instantaneous (inst) current compared to current after 3 s (both at +40 mV) for KCNQ1-KCNE1 channels in the absence (control) versus presence of MTX (30 μM). $^{**}P < 0.01$ (n = 5). Left: Raw currents. Right: Instantaneous current/3-s current. (**D**) Mean KCNQ1-KCNE1 channel deactivation rate versus voltage in the absence (control) and presence of MTX (30 μM). (**E**) Mean dose response for effects of MTX on KCNQ1-KCNE1 current magnitude at −40 mV (n = 5). (**F**) Averaged KCNQ1-KCNE3 current traces in response to voltage protocol [as in (A)] in the absence (control) or presence of 30 μM MTX (n = 8). (**G**) Mean effects of 30 μM MTX on KCNQ1 and KCNQ1-KCNE3 raw tail currents at −30 mV after prepulses as indicated [as in (F); n = 8]. (**H**) Averaged KCNQ1-KCNE4 current traces in response to voltage protocol [as in (A)] in the absence (control) or presence of 30 μM MTX (n = 5). (**I**) Mean effects of 30 μM MTX on KCNQ1 and KCNQ1-KCNE4 raw tail currents at −30 mV after prepulses as indicated [as in (H); n = 5).

at negative membrane potentials, an effect that requires the KCNQ3 S5 tryptophan W265 (*31*). Here, we found that MTX (30 μM) was ineffective at rescuing KCNQ1 from inhibition by UCL2077 at positive voltages, but still augmented KCNQ1 current at hyperpolarized voltages despite the presence of UCL2077 (10 μM) (fig. S5, C and D). This bimodal effect was reminiscent of the reported effect of UCL2077 on KCNQ3 via its W265; however, KCNQ1 lacks W265 and is generally insensitive to the augmenting effects of various agonists that augment some or all of KCNQ2-5 isoforms via the W265 equivalent (*33*–*35*). This led us to speculate that MTX might sit in a binding pocket on KCNQ1 outside the pore but close enough to S5 to influence pore conformation and/or voltage sensitivity.

MTX and CPT1 bind to KCNQ1-R243 at the foot of the voltage sensor

To elucidate the specific MTX binding site on KCNQ1, we performed unbiased in silico docking prediction analysis (SwissDock) using the recent cryo-electron microscopy (cryo-EM)–derived KCNQ1 structure (*36*). These simulations predicted that MTX binds to R243, which lies at the foot of S4, the charged helix that senses membrane potential, abutting the S4-S5 linker. Several poses exhibited hydrogen bond formation between R243 and a hydroxyl group on MTX (Fig. 5, A to C). In agreement with this prediction, mutation of KCNQ1-R243 to alanine rendered both KCNQ1 and KCNQ1-KCNE1 complexes completely insensitive to MTX (10 μM) (Fig. 5D and fig. S6). Docking simulations predicted that CPT1 also binds to KCNQ1-R243 (Fig. 5E). Accordingly, alanine substitution of KCNQ1-R243 eliminated KCNQ1 (Fig. 5F and fig. S6, E and F) and KCNQ1-KCNE1 (fig. S6, G and H) sensitivity to CPT1.

Superimposed docking simulations suggested that MTX and CPT1 would compete for the same binding site, rather than being simultaneously accommodated in the same binding pocket (Fig. 5G). Consistent with this prediction, coapplication of both MTX and CPT1 produced KCNQ1 current augmentation intermediate between

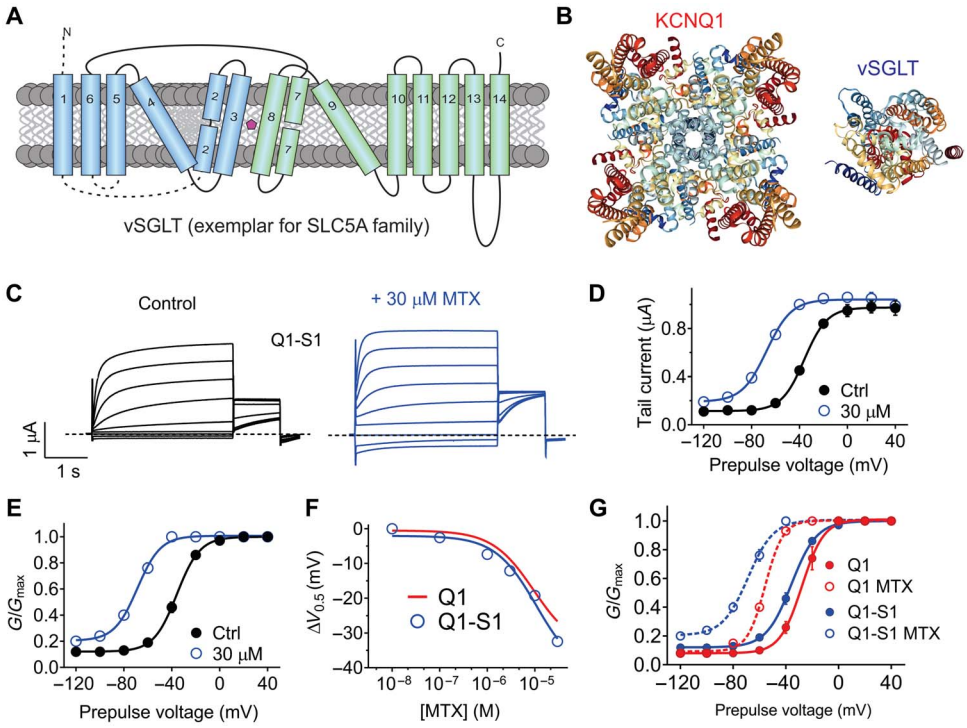

Fig. 4. Summation of effects of MTX and SMIT1 on KCNQ1 activation. All error bars indicate SEM. (**A**) Topology of vSGLT, a eukaryotic SLC5A family ortholog bearing predicted structural similarity to SMIT1. (**B**) High-resolution structures of KCNQ1 and vSGLT (extracellular view) to illustrate relative sizes. (**C**) Averaged KCNQ1-SMIT1 traces in the absence (control) or presence of 30 μM MTX (n = 5). Dashed line indicates zero current level. (**D**) Mean effects of 30 μM MTX on KCNQ1-SMIT1 raw tail currents at −30 mV after prepulses as indicated [as in (C); n = 5]. (**E**) Mean effects of 30 μM MTX on KCNQ1-SMIT1 G/G_{max} calculated from tail currents at −30 mV after prepulses as indicated [as in (C); n = 5]. (**F**) MTX dose response for mean $\Delta V_{0.5}$ of activation of KCNQ1-SMIT1 (blue) and KCNQ1 (red) (n = 5 to 7). (**G**) Comparison of mean effects of 30 μM MTX on KCNQ1 (red) and KCNQ1-SMIT1 (blue) G/G_{max} calculated from tail currents at −30 mV after prepulses as indicated [as in (C); n = 5 to 7].

that observed for similar concentrations of either compound alone (Figs. 5, H and I, and fig. S6I). Last, we tested a cocktail of the 10 *M. oppositifolius* leaf extract components shown in Fig. 1 (see Materials and Methods for individual concentrations) to determine whether this created synergistic activation of KCNQ1, but it did not; the cocktail was mildly inhibitory at depolarized potentials and slightly augmented KCNQ1 activity at hyperpolarized potentials (Fig. 5J and fig. S6J). Together, these data strongly suggest that R243 on the S4-S5 linker of KCNQ1 is the binding site for both MTX and CPT1 and that these are the primary KCNQ1-activating components of *M. oppositifolius* leaf extract.

MTX also binds to the R243 equivalent in KCNQ2/3 potassium channels

While KCNQ1 channels are essential for human ventricular myocardium repolarization and for the function of a variety of epithelia (*8*), KCNQ2/3 channels are best known for generating the muscarinic-inhibited M current, essential for regulating neuronal excitability (*37*–*39*). We recently found that MTX also activates KCNQ2/3 channels in a binding pocket associated with their S5 tryptophan (W236/W265) but not absolutely requiring it for KCNQ2/3 current augmentation (*40*). Here, in silico docking prediction and analysis of potential hydrogen bonding, using a chimeric KCNQ1/KCNQ3 model we developed using the cryo-EM–derived KCNQ1 structure (*36*, *41*), predicted that similar to the situation in KCNQ1 channels, MTX hydrogen bonds to the R243 equivalent (R213/R242) at the foot of the voltage sensor of KCNQ2/3 channels (Fig. 6, A to C). We previously found that KCNQ2 is more sensitive than KCNQ3 to MTX augmentation (*40*). Here, heteromeric channels formed from KCNQ2-R213A and wild-type KCNQ3 exhibited altered voltage dependence of MTX sensitivity, at least partly because they were less active at baseline than wild-type KCNQ2/3 at hyperpolarized voltages; at a given voltage, the mutant channels tended to exhibit a slightly greater MTX-induced shift in the $V_{0.5}$ of activation. MTX was even more efficacious upon channels formed from wild-type KCNQ2 with KCNQ3-R242A. In contrast, KCNQ2/3 channels carrying both the KCNQ2-R213A and KCNQ3-R242A substitutions ("RA-RA") were insensitive to MTX (Fig. 6, D and E, and figs. S7 to S10). Thus, as for KCNQ1, MTX binds to R213/R242 on KCNQ2/3 channels, and this is required for current augmentation.

DISCUSSION

Our findings reveal a novel mechanism for pharmacological activation of Kv channels, involving hydrogen bonding to the arginine lying between the S4-S5 linker and the voltage sensor. Results of channel voltage dependence and gating measurements suggest that MTX and CPT1 binding to KCNQ1-R243 stabilizes the channel open state and destabilizes the closed state. Ion channels in general, and arguably potassium channels in particular, represent an extremely rich vein to tap in terms of drug targets, yet progress to date has matched neither the need nor the potential. In this study, we demonstrate one example of how traditional medicines have much to offer in this regard. By deconstructing

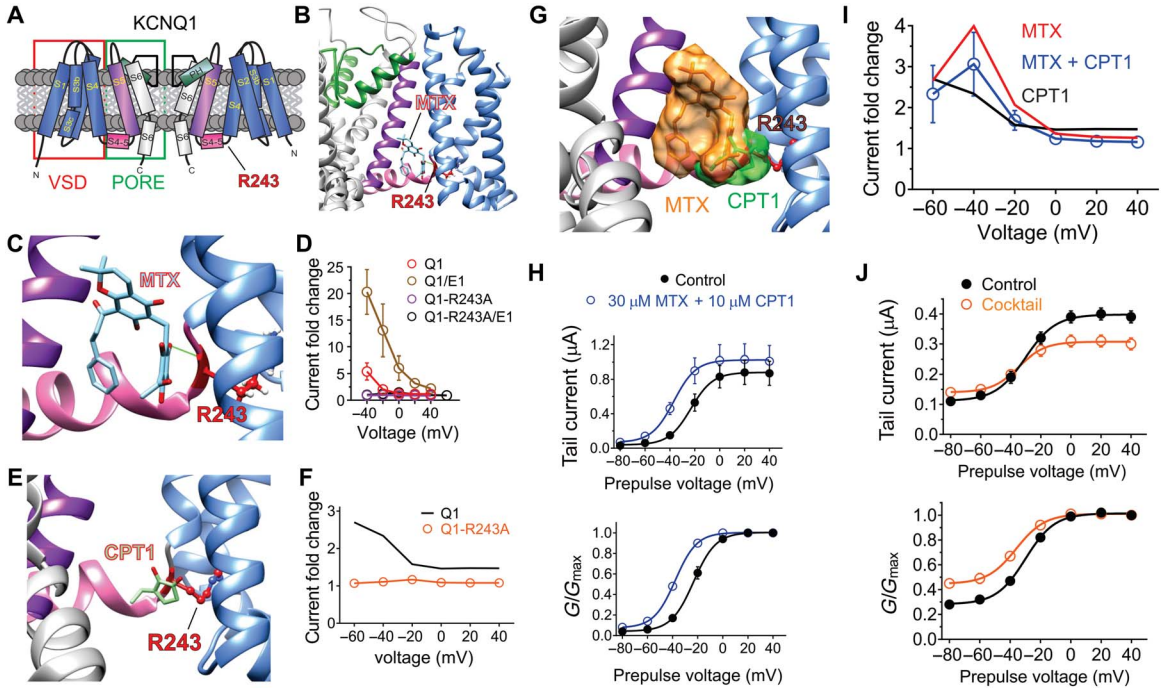

Fig. 5. MTX and CPT1 compete for binding to R243 on the KCNQ1 S4-S5 linker. All error bars indicate SEM. (**A**) KCNQ1 topology (two of four subunits shown) indicating the position of R243 on the S4-S5 linker. (**B**) SwissDock result showing predicted binding of MTX to KCNQ1 via hydrogen bonding (green line) to R243. (**C**) Close-up of docking shown in (B). (**D**) Mean current augmentation by MTX versus voltage of wild-type and KCNQ1-R243A and KCNQ1-KCNE1 channels (n = 5 to 8). (**E**) SwissDock result showing predicted binding of CPT1 to KCNQ1-R243. (**F**) Mean current augmentation by CPT1 versus voltage of wild-type (from Fig. 2) and KCNQ1-R243A channels (n = 10). (**G**) SwissDock result showing predicted binding pose overlap in KCNQ1 of MTX and CPT1. (**H**) Mean effects of 30 μM MTX + 10 μM CPT1 on KCNQ1 raw tail currents (upper) and G/G_{max} (lower) at −30 mV after prepulses as indicated (n = 5). (**I**) Mean current augmentation versus voltage of KCNQ1 by 30 μM MTX + 10 μM CPT1 (blue) [from (H)] compared to effects for MTX alone (red) or CPT1 alone (orange) (from Fig. 2) (n = 4 to 7). (**J**) Mean effects of *M. oppositifolius* leaf extract cocktail on KCNQ1 raw tail currents (upper) and G/G_{max} (lower) at −30 mV after prepulses as indicated (n = 6).

the therapeutic leaf extract of M. *oppositifolius*, we have found both a novel binding site (KCNQ1-R243) and a novel chemical space (CPT1) for Kv channel activation.

In rats fed *Mallotus philippensis* extract, oral bioavailability of MTX has been previously quantified to be >20%, while plasma concentrations have been measured in excess of 2 μg/ml. This high concentration is aided by the high concentration of MTX in *Mallotus*, which was measured to be 21% (w/w) content of a powder prepared from *M. philippensis* fruit (*42*). Plasma levels (2 μg/ml) equate to 4 μM MTX, at which concentration MTX activates homomeric KCNQ1, and more efficaciously when in complexes with KCNE1. The levels that CPT1 reaches in the plasma are not established but would not necessarily need to be very high, given that we found that CPT1 is a potent KCNQ1 activator (EC_{50} of 100 nM).

As the leaf extract has been used for centuries in folk medicine, it is tempting to assume that toxicity is low, but extensive preclinical investigations of MTX and CPT1, including toxicity testing, would be needed before moving to human trials. Like many modern medicines, MTX is toxic in large doses (*43*). By the same token, further exploration of derivatives of these two compounds might yield safer and/or more efficacious compounds better suited for drug trials. Recently, we found that two components of *M. oppositifolius* leaf extract, MTX and isovaleric acid, synergistically activated heteromeric KCNQ2/3 channels, thus uncovering the molecular mechanism behind the anticonvulsant properties of this widely used African traditional medicine (*40*). KCNQ1 lacks the S5 tryptophan, KCNQ2-W235, required for activation by isovaleric acid, and therefore is insensitive to it. However, our new data show that MTX sensitivity is shared between these KCNQs because the R243 equivalent is conserved among them. Our other recent work suggests that the S5 tryptophan is absent from the nonneuronal KCNQ1 because KCNQ3-W265 and its equivalent evolved in a neuronal progenitor KCNQ subunit to confer sensitivity to neuronal metabolites/neurotransmitters including γ-aminobutyric acid and γ-amino-β-hydroxybutyric acid (*41*). As more of the picture becomes clear of KCNQ pharmacology, with respect to endogenous and exogenous natural compounds, we will be better able to predict and develop specificity, synergy, safety, and efficacy for polypharmaceutical modulation of this influential Kv channel family.

There are many other species in the genus *Mallotus*, ranging across Africa, Asia, Afghanistan, and Australia. While some are currently primarily in ornamental use (e.g., *Mallotus japonica*), others are also used for dyes and medicinal purposes. *Mallotus philippinensis*, widely distributed along the east coast of Australia and in the Himalayas, bears glandular hairs from its fruit capsule that yield *Kamala*, a red powder used as an antihelminthic and effective in animal models of wound healing (*44*). Some, including *M. oppositifolius*, the Ghanian shrub *Mallotus atrovirens*, and the Sri Lankan shrub *Mallotus fuscescens*, are on the International Union for Conservation of Nature Red List of Threatened Species, underlining the importance of discovering therapeutic uses of the constituents of these plants and protecting them by safeguarding their natural environments.

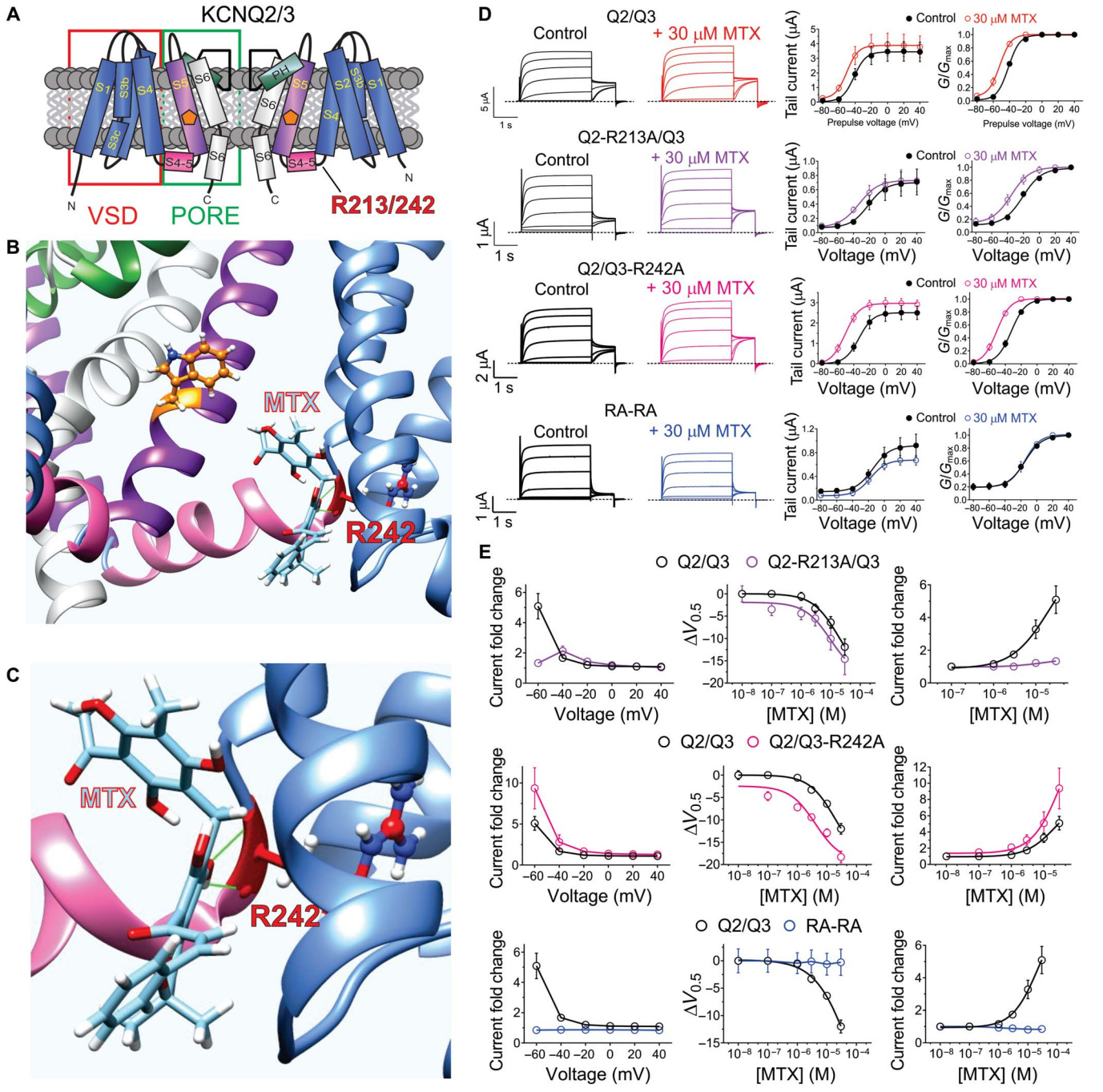

Fig. 6. MTX binds to the R243 equivalents on KCNQ2/3 channels. All error bars indicate SEM. (**A**) KCNQ2/3 topology (two of four subunits shown) indicating the position of R243 equivalents (R213/242) and of KCNQ2-W236/KCNQ3-W265 (orange pentagons). (**B**) SwissDock result showing predicted binding of MTX to KCNQ3 via hydrogen bonding (green line) to R242. (**C**) Close-up of docking shown in (B). (**D**) Left: Averaged wild-type and arginine mutant KCNQ2/3 traces as indicated in the absence (control) or presence of 30 μM MTX. Dashed line indicates zero current level. Mean tail currents (center). Mean G/G_{max} (right) from traces as in left (n = 5 to 6). (**E**) Analysis of MTX effects recorded from wild-type and mutant KCNQ2/3 traces as in (D). Left: Current fold change in response to MTX (30 μM). Center: MTX dose responses for channel $V_{0.5}$ activation shifts. Right: MTX dose responses for channel current augmentation at −60 mV (n = 5 to 6).

MATERIALS AND METHODS

Channel subunit cRNA preparation and X. laevis oocyte injection

Complementary RNA (cRNA) transcripts encoding human KCNQ1, KCNQ2, KCNQ3, KCNE1, KCNE3, KCNE4, or SMIT1 were generated by in vitro transcription using a T7 polymerase mMessage mMachine kit (Thermo Fisher Scientific), after vector linearization, from complementary DNA (cDNA) subcloned into plasmids incorporating *X. laevis* β-globin 5′ and 3′ untranslated regions flanking the coding region to enhance translation and cRNA stability. cRNA was quantified

by spectrophotometry. Mutant cDNAs were generated by site-directed mutagenesis using a QuikChange kit according to the manufacturer's protocol (Agilent, Santa Clara, CA) and corresponding cRNAs prepared as above. Commercially sourced, defolliculated stages V and VI *X. laevis* oocytes (Ecocyte Bioscience, Austin, TX) were injected with Kv channel α subunit cRNAs (10 ng total per oocyte). Oocytes were incubated at 16°C in Barth's saline solution (Ecocyte Bioscience) containing penicillin and streptomycin, with daily washing for 2 to 5 days before two-electrode voltage-clamp (TEVC) recording.

Two-electrode voltage clamp

TEVC recording was performed at room temperature with an OC-725C amplifier (Warner Instruments, Hamden, CT) and pCLAMP 8 software (Molecular Devices, Sunnyvale, CA) 2 to 5 days after cRNA injection as described in the section above. Oocytes were placed in a small-volume oocyte bath (Warner) and viewed with a dissection microscope. Chemicals were sourced from Sigma-Aldrich. Bath solution was composed of 96 mM NaCl, 4 mM KCl, 1 mM $MgCl_2$, 1 mM $CaCl_2$, and 10 mM Hepes (pH 7.6). Isovaleric acid, 2-mercaptophenol, 1-heptene, and CPT1 were stored at 4°C as 5 mM stocks in Ringer's solution. MTX (dimethyl sulfoxide), sorbic acid (ethanol), and glutaconic acid (molecular grade H_2O) were stored at −20°C as 1 M stocks. Oleamide was stored as a 1 mM stock in ethanol at 4°C. Palmitic acid was conjugated with bovine serum albumin as a 1 mM stock and stored at −20°C, as previously described (*40*). All compounds were diluted to working concentrations each experimental day. The leaf extract cocktail was composed of 10 μM MTX, 10 μM CPT1, 50 μM palmitic acid, 50 μM isovaleric acid, 50 μM valeric acid, 50 μM glutaconic acid, 50 μM sorbic acid, 50 μM 1-heptene, 50 μM 2-mercaptophenol, and 50 μM oleamide.

Compounds were introduced to the recording bath via gravity perfusion at a constant flow of 1 ml/min for 3 min prior to recording. Pipettes were of 1 to 2 megohm resistance when filled with 3 M KCl. Currents were recorded in response to pulses between −80 and +40 mV at 20-mV intervals, or a single pulse to +40 mV from a holding potential of −80 mV to yield current-voltage relationships, current magnitude, and for quantifying activation rate. TEVC data analysis was performed with Clampfit (Molecular Devices) and GraphPad Prism software (GraphPad, San Diego, CA, USA). Values are stated as mean ± SEM. Normalized tail currents were plotted versus prepulse voltage and fitted with a single Boltzmann function

$$g = \frac{(A_1 - A_2)}{\left\{1 + \exp\left[V_{\frac{1}{2}} - V\right]\right\}y + A_2} \quad (1)$$

where g is the normalized tail conductance, A_1 is the initial value at $-\infty$, A_2 is the final value at $+\infty$, $V_{1/2}$ is the half-maximal voltage of activation, and V_s is the slope factor. Activation and deactivation kinetics were fitted with single exponential functions.

Chemical structures, in silico docking, and sequence analyses

Chemical structures and electrostatic surface potentials (range, −0.1 to 0.1) were plotted using Jmol, an open-source Java viewer for chemical structures in three dimension (http://jmol.org/). Unguided docking of MTX and CPT1 to predict binding sites was performed using the *X. laevis* KCNQ1 cryo-EM structure (*36*) and a KCNQ1-KCNQ3 chimeric model based on it (*41*) using SwissDock (*45*) with CHARMM (Chemistry at HARvard Macromolecular Mechanics) force fields (*46*), as previously described (*47*).

Statistical analysis

All values are expressed as mean ± SEM. All P values were two sided. Statistical significance was defined as $P < 0.05$.

SUPPLEMENTARY MATERIALS

Supplementary material for this article is available at http://advances.sciencemag.org/cgi/content/full/4/11/eaav0824/DC1

Fig. S1. Effects of CPT1 on KCNQ1 channels.
Fig. S2. Effects of MTX on KCNQ1 channels.
Fig. S3. Effects of MTX on KCNQ1/KCNE1 channels.
Fig. S4. Effects of MTX on KCNQ1/SMIT1 channels.
Fig. S5. Interaction of MTX with permeant ions and UCL2077.
Fig. S6. MTX and CPT1 bind to R243 on the KCNQ1 S4-S5 linker.
Fig. S7. Effects of MTX on KCNQ2/KCNQ3 channels.
Fig. S8. Effects of MTX on KCNQ2-R213A/KCNQ3 channels.
Fig. S9. Effects of MTX on KCNQ2/KCNQ3-R242A channels.
Fig. S10. Effects of MTX on KCNQ2-R213A/KCNQ3-R242A channels.

REFERENCES AND NOTES

1. World Health Organization, *The World Medicines Situation*, (World Health Organization, 2004); http://apps.who.int/medicinedocs/pdf/s6160e/s6160e.pdf.
2. A. A. Adekunle, Ethnobotanical studies of some medicinal plants from Lagos State of Nigeria. *Niger. J. Bot.* **14**, 71–79 (2001).
3. H. M. Burkhill, *The Useful Plants of West Tropical Africa*. (Royal Botanic Gardens, Kew, 1994), vol. 2, pp. 636.
4. A. A. Adekunle, A. M. Ikumapayi, Antifungal property and phytochemical screening of the crude extracts of *Funtumia elastica* and *Mallotus oppositifolius*. *West Indian Med. J.* **55**, 219–223 (2006).
5. V. Matschke, I. Piccini, J. Schubert, E. Wrobel, F. Lang, J. Matschke, E. Amedonu, S. G. Meuth, T. Strünker, N. Strutz-Seebohm, B. Greber, J. Scherkenbeck, G. Seebohm, The natural plant product rottlerin activates Kv7.1/KCNE1 channels. *Cell. Physiol. Biochem.* **40**, 1549–1558 (2016).
6. S. I. Zakharov, J. P. Morrow, G. Liu, L. Yang, S. O. Marx, Activation of the BK (SLO1) potassium channel by mallotoxin. *J. Biol. Chem.* **280**, 30882–30887 (2005).
7. H. Zeng, I. M. Lozinskaya, Z. Lin, R. N. Willette, D. P. Brooks, X. Xu, Mallotoxin is a novel human *ether-a-go-go*-related gene (hERG) potassium channel activator. *J. Pharmacol. Exp. Ther.* **319**, 957–962 (2006).
8. G. W. Abbott, Biology of the KCNQ1 potassium channel. *New J. Sci.* **2014**, 1–26 (2014).
9. M. W. Russell, M. Dick II, F. S. Collins, L. C. Brody, KVLQT1 mutations in three families with familial or sporadic long QT syndrome. *Hum. Mol. Genet.* **5**, 1319–1324 (1996).
10. J. Tyson, L. Tranebjærg, S. Bellman, C. Wren, J. F. N. Taylor, J. Bathen, B. Aslaksen, S. J. Sørland, O. Lund, S. Malcolm, M. Pembrey, S. Bhattacharya, M. Bitner-Glindzicz, IsK and KvLQT1: Mutation in either of the two subunits of the slow component of the delayed rectifier potassium channel can cause Jervell and Lange-Nielsen syndrome. *Hum. Mol. Genet.* **6**, 2179–2185 (1997).
11. Y.-H. Lee, E. S. Kang, S. H. Kim, S. J. Han, C. H. Kim, H. J. Kim, C. W. Ahn, B. S. Cha, M. Nam, C. M. Nam, H. C. Lee, Association between polymorphisms in *SLC30A8*, *HHEX*, *CDKN2A/B*, *IGF2BP2*, *FTO*, *WFS1*, *CDKAL1*, *KCNQ1* and type 2 diabetes in the Korean population. *J. Hum. Genet.* **53**, 991–998 (2008).
12. H. Unoki, A. Takahashi, T. Kawaguchi, K. Hara, M. Horikoshi, G. Andersen, D. P. K. Ng, J. Holmkvist, K. Borch-Johnsen, T. Jørgensen, A. Sandbæk, T. Lauritzen, T. Hansen, S. Nurbaya, T. Tsunoda, M. Kubo, T. Babazono, H. Hirose, M. Hayashi, Y. Iwamoto, A. Kashiwagi, K. Kaku, R. Kawamori, E. S. Tai, O. Pedersen, N. Kamatani, T. Kadowaki, R. Kikkawa, Y. Nakamura, S. Maeda, SNPs in *KCNQ1* are associated with susceptibility to type 2 diabetes in East Asian and European populations. *Nat. Genet.* **40**, 1098–1102 (2008).
13. K. Yasuda, K. Miyake, Y. Horikawa, K. Hara, H. Osawa, H. Furuta, Y. Hirota, H. Mori, A. Jonsson, Y. Sato, K. Yamagata, Y. Hinokio, H.-Y. Wang, T. Tanahashi, N. Nakamura, Y. Oka, N. Iwasaki, Y. Iwamoto, Y. Yamada, Y. Seino, H. Maegawa, A. Kashiwagi, J. Takeda, E. Maeda, H. D. Shin, Y. M. Cho, K. S. Park, H. K. Lee, M. C. Y. Ng, R. C. W. Ma, W.-Y. So, J. C. N. Chan, V. Lyssenko, T. Tuomi, P. Nilsson, L. Groop, N. Kamatani, A. Sekine, Y. Nakamura, K. Yamamoto, T. Yoshida, K. Tokunaga, M. Itakura, H. Makino, K. Nanjo, T. Kadowaki, M. Kasuga, Variants in *KCNQ1* are associated with susceptibility to type 2 diabetes mellitus. *Nat. Genet.* **40**, 1092–1097 (2008).
14. K. S. Rice, G. Dickson, M. Lane, J. Crawford, S.-K. Chung, M. I. Rees, A. N. Shelling, D. R. Love, J. R. Skinner, Elevated serum gastrin levels in Jervell and Lange-Nielsen syndrome: A marker of severe KCNQ1 dysfunction? *Heart Rhythm* **8**, 551–554 (2011).

15. A. Winbo, O. Sandstrom, R. Palmqvist, A. Rydberg, Iron-deficiency anaemia, gastric hyperplasia, and elevated gastrin levels due to potassium channel dysfunction in the Jervell and Lange-Nielsen Syndrome. *Cardiol. Young* **23**, 325–334 (2013).
16. H. Frohlich, K. M. Boini, G. Seebohm, N. Strutz-Seebohm, O. N. Ureche, M. Föller, M. Eichenmüller, E. Shumilina, G. Pathare, A. K. Singh, U. Seidler, K. E. Pfeifer, F. Lang, Hypothyroidism of gene-targeted mice lacking Kcnq1. *Pflugers Arch.* **461**, 45–52 (2011).
17. A. M. Neal, H. C. Taylor, I. D. Millar, J. D. Kibble, S. J. White, L. Robson, Renal defects in KCNE1 knockout mice are mimicked by chromanol 293B in vivo: Identification of a KCNE1-regulated K^+ conductance in the proximal tubule. *J. Physiol.* **589**, 3595–3609 (2011).
18. K. K. Igwe, A. J. Madubuike, I. E. Otuokere, F. J. Amaku, I. Chika, GC-MS analysis for structural identification and bioactive compounds in methanolic leaf extract of *Mallotus oppositifolius*. *Int. J. Sci. Res. Manage.* **4**, 4123–4129 (2016).
19. I. Splawski, K. W. Timothy, G. M. Vincent, D. L. Atkinson, M. T. Keating, Molecular basis of the long-QT syndrome associated with deafness. *N. Engl. J. Med.* **336**, 1562–1567 (1997).
20. G. C. L. Bett, M. J. Morales, D. L. Beahm, M. E. Duffey, R. L. Rasmusson, Ancillary subunits and stimulation frequency determine the potency of chromanol 293B block of the KCNQ1 potassium channel. *J. Physiol.* **576**, 755–767 (2006).
21. Z. Gao, Q. Xiong, H. Sun, M. Li, Desensitization of chemical activation by auxiliary subunits: Convergence of molecular determinants critical for augmenting KCNQ1 potassium channels. *J. Biol. Chem.* **283**, 22649–22658 (2008).
22. E. Choi, G. W. Abbott, A shared mechanism for lipid- and β-subunit-coordinated stabilization of the activated K^+ channel voltage sensor. *FASEB J.* **24**, 1518–1524 (2010).
23. G. Panaghie, G. W. Abbott, The role of S4 charges in voltage-dependent and voltage-independent KCNQ1 potassium channel complexes. *J. Gen. Physiol.* **129**, 121–133 (2007).
24. B. C. Schroeder, S. Waldegger, S. Fehr, M. Bleich, R. Warth, R. Greger, T. J. Jentsch, A constitutively open potassium channel formed by KCNQ1 and KCNE3. *Nature* **403**, 196–199 (2000).
25. S. Bendahhou, C. Marionneau, K. Haurogne, M.-M. Larroque, R. Derand, V. Szuts, D. Escande, S. Demolombe, J. Barhanin, In vitro molecular interactions and distribution of KCNE family with KCNQ1 in the human heart. *Cardiovasc. Res.* **67**, 529–538 (2005).
26. S. Radicke, D. Cotella, E. M. Graf, U. Banse, N. Jost, A. Varró, G.-N. Tseng, U. Ravens, E. Wettwer, Functional modulation of the transient outward current *I*to by KCNE β-subunits and regional distribution in human non-failing and failing hearts. *Cardiovasc. Res.* **71**, 695–703 (2006).
27. S. M. Crump, Z. Hu, R. Kant, D. I. Levy, S. A. N. Goldstein, G. W. Abbott, *Kcne4* deletion sex- and age-specifically impairs cardiac repolarization in mice. *FASEB J.* **30**, 360–369 (2016).
28. M. Grunnet, T. Jespersen, H. B. Rasmussen, T. Ljungstrøm, N. K. Jorgensen, S.-P. Olesen, D. A. Klaerke, KCNE4 is an inhibitory subunit to the KCNQ1 channel. *J. Physiol.* **542**, 119–130 (2002).
29. M. Grunnet, S.-P. Olesen, D. A. Klaerke, T. Jespersen, hKCNE4 inhibits the hKCNQ1 potassium current without affecting the activation kinetics. *Biochem. Biophys. Res. Commun.* **328**, 1146–1153 (2005).
30. R. W. Manville, D. L. Neverisky, G. W. Abbott, SMIT1 modifies KCNQ channel function and pharmacology by physical interaction with the pore. *Biophys. J.* **113**, 613–626 (2017).
31. H. Soh, A. V. Tzingounis, The specific slow afterhyperpolarization inhibitor UCL2077 is a subtype-selective blocker of the epilepsy associated KCNQ channels. *Mol. Pharmacol.* **78**, 1088–1095 (2010).
32. G. Peng, R. Barro-Soria, K. J. Sampson, H. P. Larsson, R. S. Kass, Gating mechanisms underlying deactivation slowing by two KCNQ1 atrial fibrillation mutations. *Sci. Rep.* **7**, 45911 (2017).
33. L. Tatulian, P. Delmas, F. C. Abogadie, D. A. Brown, Activation of expressed KCNQ potassium currents and native neuronal M-type potassium currents by the anti-convulsant drug retigabine. *J. Neurosci.* **21**, 5535–5545 (2001).
34. T. V. Wuttke, G. Seebohm, S. Bail, S. Maljevic, H. Lerche, The new anticonvulsant retigabine favors voltage-dependent opening of the $K_v7.2$ (*KCNQ2*) channel by binding to its activation gate. *Mol. Pharmacol.* **67**, 1009–1017 (2005).
35. W. Lange, J. Geißendörfer, A. Schenzer, J. Grötzinger, G. Seebohm, T. Friedrich, M. Schwake, Refinement of the binding site and mode of action of the anticonvulsant Retigabine on KCNQ K^+ channels. *Mol. Pharmacol.* **75**, 272–280 (2009).
36. J. Sun, R. MacKinnon, Cryo-EM structure of a KCNQ1/CaM complex reveals insights into congenital long QT syndrome. *Cell* **169**, 1042–1050.e9 (2017).
37. B. C. Schroeder, C. Kubisch, V. Stein, T. J. Jentsch, Moderate loss of function of cyclic-AMP-modulated KCNQ2/KCNQ3 K^+ channels causes epilepsy. *Nature* **396**, 687–690 (1998).
38. N. A. Singh, C. Charlier, D. Stauffer, B. R. DuPont, R. J. Leach, R. Melis, G. M. Ronen, I. Bjerre, T. Quattlebaum, J. V. Murphy, M. L. McHarg, D. Gagnon, T. O. Rosales, A. Peiffer, V. E. Anderson, M. Leppert, A novel potassium channel gene, KCNQ2, is mutated in an inherited epilepsy of newborns. *Nat. Genet.* **18**, 25–29 (1998).
39. H.-S. Wang, Z. Pan, W. Shi, B. S. Brown, R. S. Wymore, I. S. Cohen, J. E. Dixon, D. McKinnon, KCNQ2 and KCNQ3 potassium channel subunits: Molecular correlates of the M-channel. *Science* **282**, 1890–1893 (1998).
40. R. W. Manville, G. W. Abbott, Ancient and modern anticonvulsants act synergistically in a KCNQ potassium channel binding pocket. *Nat. Commun.* **9**, 3845 (2018).
41. R. W. Manville, M. Papanikolaou, G. W. Abbott, Direct neurotransmitter activation of voltage-gated potassium channels. *Nat. Commun.* **9**, 1847 (2018).
42. R. K. Patel, V. R. Patel, M. G. Patel, Development and validation of a RP-HPLC method for the simultaneous determination of Embelin, Rottlerin and Ellagic acid in Vidangadi churna. *J. Pharm. Anal.* **2**, 366–371 (2012).
43. L. S. de Padua, N. Bunyapraphatsara, R. H. M. J. Lemmens, *Plant Resources of South-East Asia No. 12: Medicinal and Poisonous Plants 1*, (Backhuys Publishers, 1999), pp. 713.
44. M. Gangwar, M. K. Gautam, S. Ghildiyal, G. Nath, R. K. Goel, *Mallotus philippinensis* Muell. Arg fruit glandular hairs extract promotes wound healing on different wound model in rats. *BMC Complement. Altern. Med.* **15**, 123 (2015).
45. A. Grosdidier, V. Zoete, O. Michielin, SwissDock, a protein-small molecule docking web service based on EADock DSS. *Nucleic Acids Res.* **39**, W270–W277 (2011).
46. A. Grosdidier, V. Zoete, O. Michielin, Fast docking using the CHARMM force field with EADock DSS. *J. Comput. Chem.* **32**, 2149–2159 (2011).
47. R. W. Manville, G. W. Abbott, Gabapentin is a potent activator of KCNQ3 and KCNQ5 potassium channels. *Mol. Pharmacol.* **94**, 1155–1163 (2018).

Acknowledgments: We are grateful to G. Panaghie (Weill-Cornell Medical College, NY) for generating some of the mutant channel constructs. **Funding:** This study was supported by the NIH (GM115189 to G.W.A.). **Author contributions:** A.M.D.S. performed the oocyte experiments, analyzed the data, and edited the manuscript. R.W.M. conceived the study, performed the oocyte experiments and in silico docking, analyzed the data, co-wrote the manuscript, and prepared the figures. G.W.A. oversaw the electrophysiological studies, performed in silico docking, co-wrote the manuscript, and prepared the figures. **Competing interests:** The authors declare that they have no competing interests. **Data and materials availability:** All data needed to evaluate the conclusions in the paper are present in the paper, the Supplementary Materials, and/or the Dryad data repository (doi:10.5061/dryad.97p31jr). Additional data related to this paper may be requested from the authors.

Submitted 12 August 2018
Accepted 18 October 2018
Published 14 November 2018
10.1126/sciadv.aav0824

Citation: A. M. De Silva, R. W. Manville, G. W. Abbott, Deconstruction of an African folk medicine uncovers a novel molecular strategy for therapeutic potassium channel activation. *Sci. Adv.* **4**, eaav0824 (2018).